ENG. Struct. Civ. Eng. 2026, 20(4): 828–844
https://doi.org/10.1007/s11709-026-1298-4

RESEARCH ARTICLE

Study on the effect of pore air pressure on the existence form of water in soil during the cooling process

Pan LI[a,b], Jinfeng XU[c,d*], Haitao YU[d]

[a] *School of Civil Engineering, Sun Yat-Sen University & State Key Laboratory for Tunnel Engineering, Guangzhou 510275, China*
[b] *Southern Marine Science and Engineering Guangdong Laboratory (Zhuhai), Zhuhai 519082, China*
[c] *School of Civil Engineering and Transportation, South China University of Technology, Guangzhou 510641, China*
[d] *Department of geotechnical engineering, College of Civil Engineering, Tongji University, Shanghai 200092, China*
[*] *Corresponding author. E-mail: xujinfeng96@163.com*

ABSTRACT The reduction on the soil temperature by extreme low temperature in natural or artificial cooling methods can prompt a transformation in the existing form of water in soil and further a change in soil properties. This study is inspired by the interesting phenomenon of increased volume in frozen soils before the free water phase transition in a closed environment test. The influence mechanism of pore air pressure on the existence form of water in the soil is revealed and the viewpoint of converting bound water into free water before the free water phase transition has been proposed based on the hypothesis, theoretical analysis, numerical calculations, and experiments. The main research findings are as follows: 1) the first time discovery of the volume increment before the freezing phase transition of free water; 2) the calculation on the value of pore air pressure that can cause the transformation of the water existence form in the soil, i.e., the transformation of bound water into free water; 3) determination on the correlation between the temperature field and the initial water content. This research, which has never been investigated from this aspect, could provide an expansion on the freezing mechanism and freezing theory of soil.

KEYWORDS permafrost, free water, bound water, phase transition, pore air pressure

1 Introduction

The cold natural environment can reduce the temperature of the soil on the surface. A decrease in soil temperature leads to freezing and thawing to some extent and meanwhile an enhancement on soil strength. The freezing and swelling or thawing of the soil can have adverse effects on buildings, such as building tilting, pavement freezing and cracking, structural frost damage, and other adverse effects [1–6]. However, the reduced soil temperatures caused by natural phenomenon can increase soil strength and form absolute water-sealing curtains through refrigeration. Under this circumstance, positive values can be created. Compared to natural refrigeration, artificial ground freezing (AGF) refers to the technology that freezes water within the soil by transforming loose water-bearing rock and soil into solid frozen soil, leading to an enhancement on its strength and isolation of groundwater [7]. This technique allows underground construction to be carried out under the protection of the freezing wall [8–10]. The freezing method, at present, is widely used in the mining sectors worldwide, as well as in major projects such as tunnel access holes and liaison passages [11–13]. With a 300-year engineering application in history since its invention, a plethora of theoretical studies on permafrost have been carried out [14–18]. However, in a great deal of practical engineering projects, freezing designs are becoming more conservative and have longer freezing time [19–22]. The current serious disconnection between theoretical perceptions of permafrost and engineering practice suggests the urgency for further exploration on freezing mechanisms.

The theoretical basis of the freezing method is mainly derived from the science of permafrost, a sub discipline

Article history: Received Aug 6, 2025; Accepted Nov 14, 2025

of soil science. Soil freezing is the process of phase transition of water in the soil with the release of latent heat at the same time. The phase transition freezing of water belongs to microphysics [23,24]. Microphysical studies have shown that water has been found to exist in at least 18 phases [25], primarily influenced by temperature and pressure [26,27]. In soil science and its sub-disciplines, the existence form of water in the soil is mainly classified into four phases-free water, weakly bound water (film water), strongly bound water (adsorbed water), and pore vapor [28,29]. In this field of study, the examination of factors impacting the existence form of water has centered on temperature and the adsorption of mineral particles, among other factors [30–34]. Numerous studies have pointed out that the phase transition freezing temperatures of free, weakly bound, and strongly bound water in soil are around 0, −15, and −78 °C, respectively [35–38]. The freezing method, a sub-discipline of permafrost, is strictly allied with the theory of permafrost. Permafrost and the freezing method, which mainly uses drying tests to study the process and amount of water loss by heating the soil [39,40] has largely ignored the effect of pressure or pore air pressure on the existence form of water. External load is only one of the macroscopic forms of pressure. So far, in soil science and the following sub-disciplines, pore air pressure has been ignored and no studies on the effect of pore pressure on permafrost temperature have been found. Likewise, the effect of pressure or pore air pressure on the existence form of water in soil has also been ignored. The mechanism of the effect of pore air pressure on the temperature field remains to be explored by further studies.

Currently, the consensus on soil cooling is that only free and partially weakly bound water are involved in freezing, while strongly bound water is not involved in this process [41]. This furthers the agreement that the frost heave (volume gain of soil) is thought to be caused by the phase transition of free and partially weakly bound water, and the volume gain of soil should mainly occur during the phase transition of free water [42].

In this study, the interesting phenomenon has been discovered in the closed environment freezing test in terms of the soil volume increment. It occurs not only in the phase transition stage, but before it as well. The mechanism of pore air pressure on the existence form of water is revealed, and the perspective theory that the bound water is transformed into free water before the free water phase transition under cooling is proposed through hypothesis, theoretical analysis, numerical calculation and indoor tests. To verify this discovery, a freezing test in a closed environment was conducted and the unified curve of frost heave amount-temperature-time was established, and two findings were revealed: the existence of a large volume increment before the free water phase transition freezing and the longer phase transition plateau period at the lower soil temperature. Accordingly, the hypothesis that the pore air pressure decreasing with the decline of soil temperature will in turn lead to the conversion of bound water to free water before the free water phase transition is proposed. Then, the classical isothermal adsorption test was reformulated by using a pressure approach, revealing the mechanism of pore air pressure on the existence form of water in mineral particles. Next, the pore air pressures of naturally and artificially cooled soil were analyzed, combined with the pore pressure formulation of the classical isothermal adsorption test. A theoretical mechanism is revealed for the reduction of pore air pressure due to soil cooling, which in turn leads to the conversion of bound water into free water and the occurrence of a volume increment prior to the free water phase transition. Finally, the above hypothesis is verified by studying the permafrost temperature development pattern with the setting on only free water or only bound water.

2 Interesting phenomena and conjectures of closed environment freezing tests

The amount of frost heave and soil temperature are important elements of freezing test studies. There are few freezing tests that monitor the amount of frozen heave and soil temperature in real time, and no time-dependent frozen heave and soil temperature studies have been found. In this section, the freezing test in a closed environment [43] is rearranged to establish the relationship curve of frost heave amount-soil temperature-time, which reveals the existence of a large volume increment before free water phase transition freezing.

2.1 Overview of the experiment

The test is designed to be a closed environment, a one-way freezing test without external water replenishment. As shown in Fig. 1, the measurement of the model box is 90 cm × 60 cm × 80 cm, and the insulation material is attached externally around the model box and at the bottom. The refrigeration end was at the top of the model box, and three levels of −10, −15 and −20 °C were used respectively.

The test was carried out on loess from the Jiuzhoutai area, Lanzhou City, China, with a specific gravity of 2.71, a liquid limit of 28.38%, a plastic limit of 15.21%, an optimum water content of 13.41%, a porosity of 0.4, and a maximum dry density of 1.78 g/cm^3. 16% water content remolded soil specimens were prepared according to geotechnical test standards. In addition, the initial degree of filling of pores with water is 0.6 and mineral composition for loess of Jiuzhoutai is shown in Table 1.

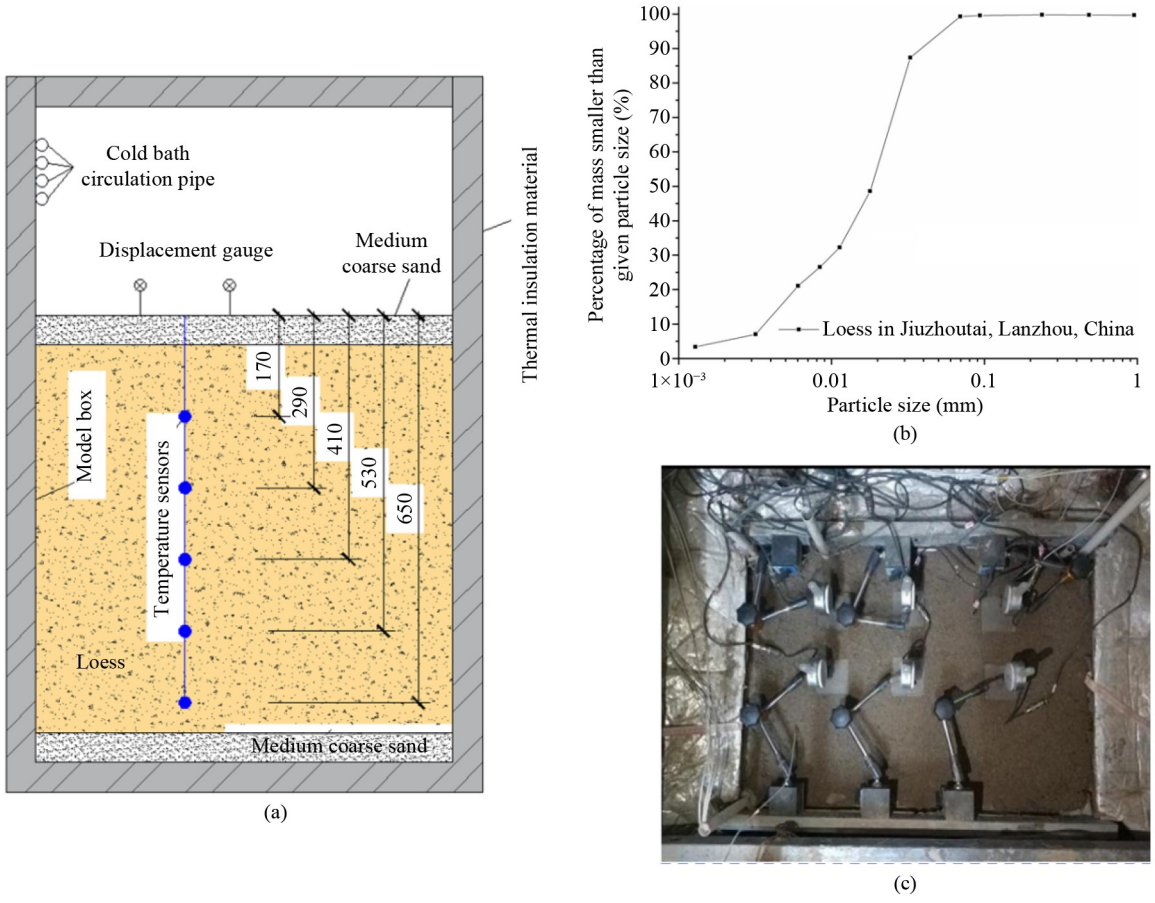

Fig. 1 Freezing test in a closed environment of loess in Lanzhou: (a) temperature measurement point location; (b) the distribution of particles by size for loess in Jiuzhoutai area; (c) measurement point location of Frost heaving amount.

Table 1 Mineral composition for loess of Jiuzhoutai

Minerals composition	Proportion (%)
Quartz	40
Microplagioclase	6
Plagioclase	13
Calcite	15
Amphibole	6
Dolomite	2
Clay mineral	18

As shown in Fig. 1, the tests were conducted to monitor the amount of frost heave and soil temperature. The temperature sensor located on the top surface, were 17, 29, 41, 53, and 65 cm (Fig. 1(a)). And data on the distribution of particles by size is shown in Fig. 1(b). Frost heaving amount sensors, located on the top surface of the specimen, six groups of different positions of frost heaving amount monitoring position are shown in Fig. 1(c). In addition, as shown in Fig. 1(a), it should be noted that this experiment was carried out in a closed low-temperature test chamber, isolated from external heat exchange and moisture exchange. In addition, since the chiller was located above the soil body and a 5 cm thick medium-coarse sand bedding layer was laid below the soil body, there was no moisture accumulation in the upper layer of the sample. Last but not least, since the chiller was located above the soil body and a 5 cm thick medium-coarse sand bedding layer was laid below the soil body, there was no moisture accumulation in the upper layer of the sample.

2.2 Frost heave amount−temperature−time uniform curve

As shown in Figs. 2(a) and 2(c), the frost heave amount-soil temperature-time change curves are plotted for cooling temperatures of −10, −15 and −20 °C. The left number axis is the volume increment (unit: mm), the right number axis is the temperature (unit: °C) and the horizontal axis is the time (unit: h). As shown in Fig. 1(a), the experiment is carried out in a low-temperature test box to safeguard the external isolation of heat exchange. Different refrigeration temperatures −10, −15, −20 °C, respectively. And cooling is carried out by means of a cold bath circulating tube, located in a space at one end of the insulated box. The maintenance temperatures −10, −15 and −20 °C were maintained throughout the experiment. In addition, it should be noted that the temperature sensor used is platinum thermistor pt100 and

its working range is −50–200 °C, precision is 0.1 °C. The frequency of temperature measurement in the experiment is 10 min each time, and the measurement time is longer than 300 h. Therefore, this experiment has enough temperature data. As shown in Fig. 2, each temperature curve contains at least 1800 data points, and the highlighted markers are selected feature points. Therefore, enough temperature data can track the temperature of supercooling of pore moisture and the temperature of the onset of freezing.

Although the above refrigeration temperatures were −10, −15, −20 °C, the lowest temperature of the test soil was −11 °C. According to the phase transition freezing temperatures of free water, weakly bound water, and strongly bound water in the soil, only free water undergoes phase transition freezing in this freezing test, and there is no phase transition freezing of bound water.

2.3 Interesting phenomenon

1) The pattern of temperature change

As shown in Fig. 2, the changes in temperature-time curves for the three conditions can be divided into three stages respectively: a sharp decrease zone, an approximate plateau decrease zone and a general decrease zone. In the first stage, the reason for the sharp decrease in temperature is the gradual cooling of the components within the soil, including unfrozen soil and unfrozen water, by releasing heat. Since a relative stability have been shown through, the temperature change pattern was

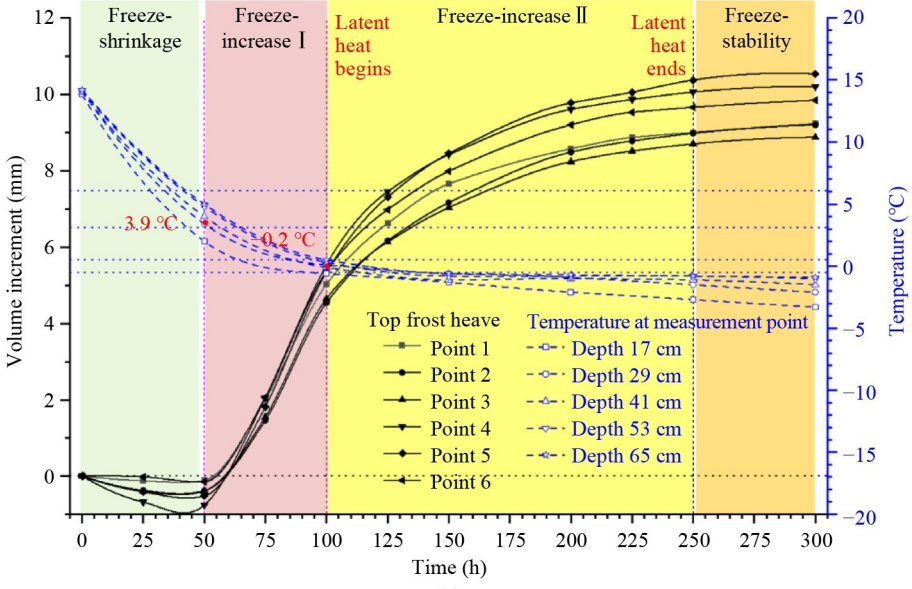

(a)

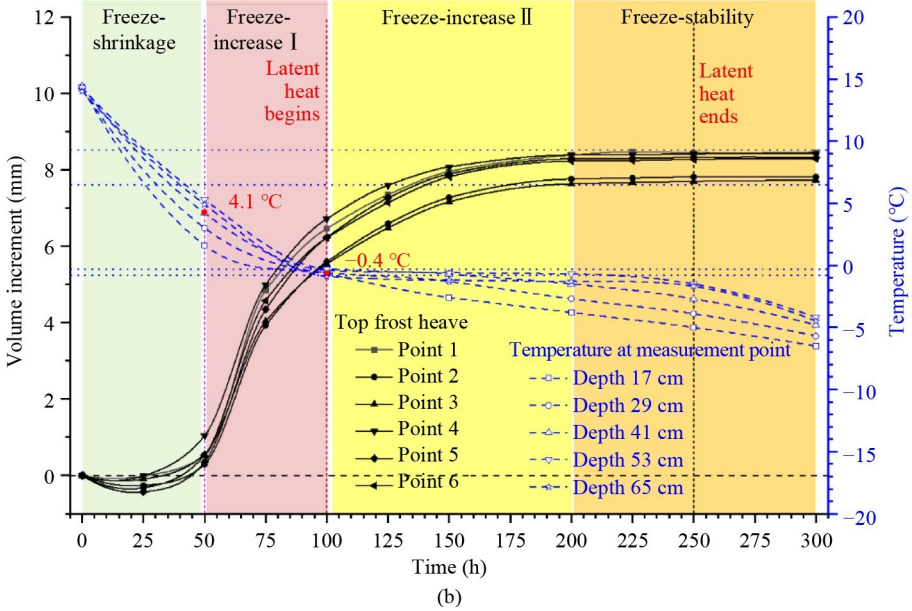

(b)

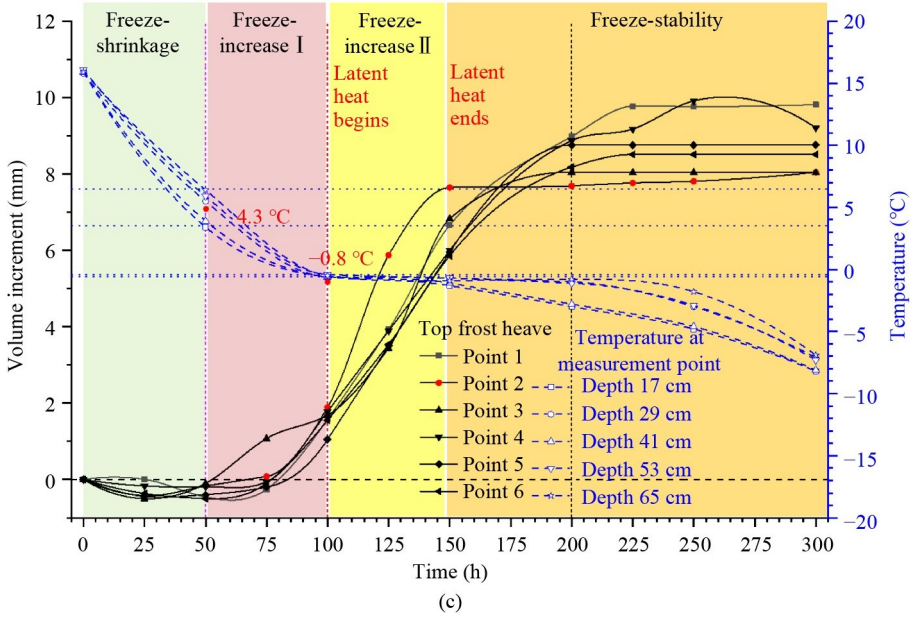

(c)

Fig. 2 Frost heave amount-temperature-time variation curves for different working conditions: (a) working condition 1: 16% water content, temperature load −10 °C; (b) working condition 2: 16% water content, temperature load −15 °C; (c) working condition 3: 16% water content, temperature load −20 °C.

consistent with time in this stage, for the approximate linear rapid decline. In the second stage, the approximate platform temperature decline is caused by the gradual release of latent heat in the free water then phase transition freezing occurs. When the latent heat released from free water phase transition encountered against the outside part of the cold, the declining rate of temperature was slow, and even into the platform period. In the third stage, when the free water phase transition freezing was close to completion or has been completed, the specific heat capacity and thermal conductivity of the ice became relatively stable, and the decreasing rate of temperature of the soil body was also approximate to a straight line. In addition, the temperature at which the temperature-time curve appeared to inflect (the starting point of the latent heat of phase change, i.e., the freezing temperature or freezing point) is about −0.8 to −0.2 °C. The lower the refrigeration temperature, the lower the freezing point temperature, but the difference was not significant.

The soil sample temperatures at the middle of the test chamber for different operating conditions are shown in Fig. 3. The different refrigeration temperature levels caused similar cooling temperature change curves. First, the first inflection point of temperature−time curve was almost the same and the time of occurrence was almost the same at different refrigeration conditions, and the difference of freezing temperature was no more than 0.4 °C and the time difference was no more than 5 h. However, the length of the plateau period for different refrigeration working conditions showed marked difference. Among them, latent heat platform period in the phase transition was about 125 h for condition 1, 75 h for condition 2, and 35 h for condition 3. In addition, the

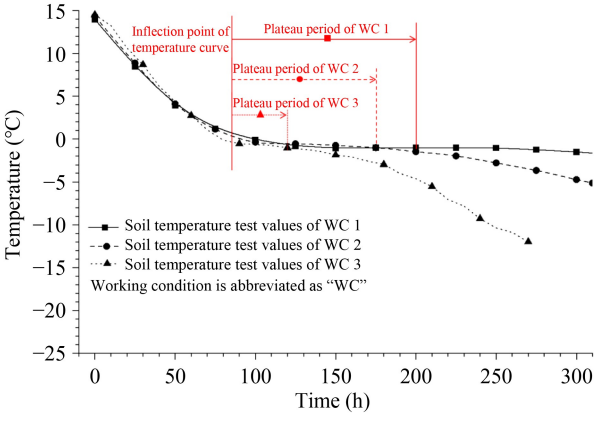

Fig. 3 Temperature development law of soil body for different working conditions.

final temperatures of the soil were significantly different under the different cooling conditions. In particular, the final soil temperature was −3.7 °C for condition 1, −5.1 °C for condition 2, and −11.9 °C for condition 3.

The above phenomenon show that the amount of water involved in the phase transition latent heat of freezing varies in different refrigeration conditions. The lower the refrigeration temperature, the more water involved in the phase transition latent vice versa. On the contrary, the higher the refrigeration temperature, the less the amount of water involved in freezing, the longer the phase transition latent heat platform period, and the higher the final temperature. Therefore, in a closed environment, without external moisture infiltration into the interior, it is necessary to further reveal the reasons for the different amounts of water involved in the latent heat of phase

transition at different refrigeration temperatures.

2) Pattern of change in volume increment

The pattern of change of volume increment of soil with time under general cooling is divided into three stages: freeze-shrinkage zone, freeze-increase zone and freeze-stability zone. For cohesive soils, the existence of freeze-shrinkage zone is believed to be caused by the shrinkage of soil particles due to cooling [44], and this perception is contradicted by the smaller effect of temperature change on the bilayer potential of mineral particles [45]. An agreement has been reached on both the freezing-increase and freeze-stability zones: the former occurs when the moisture in the soil body undergoes a phase transition to freezing. The later is caused by the complete phase transition freezing in the moisture in the soil body and no longer causes a significant increase in the frost heave amount. A single analysis of the soil volume increment-time curve will clearly demonstrate that there is only one freezing- increase zone due to free water phase transition freezing.

Under this closed environment test, the volume increment of the soil can be only caused by the phase transition freezing of the original free water in the soil. The volume increment of the soil should only occur in the stage of free water phase transition freezing, in the zone of temperature approximate plateau drop. However, when the frost heave amount-time curve is combined with the temperature-time change curve (Fig. 2), it is found that taking the time of the starting point of free water phase transition freezing as the node-freezing increase zone can be divided into two parts: the stage before free water freezing increase zone and the stage of free water freezing increase zone. The volume increment before the phase transition of free water occurs (hereinafter referred to as the freezing increase zone I), and the volume increment during the free water phase transition freezing stage (hereinafter referred to as the freezing increase zone II). In the above three conditions, the ratio of the frost heave amount increment between the freezing increase zone I and the freezing increase zone II was about 1.1:1, 2.0:1, and 4.7:1, respectively. The volume increment between the free water phase transition accounted for about 52%, 67%, and 82% of the total volume increment. The volume increment before the free water phase transition should not be ignored and even exceeds the volume increment during the free water phase transition freezing stage. As the soil temperature gets lower, the proportion of the total volume increment increases.

2.4 Conjectures

Given that the influence of external moisture migration is excluded under a closed environment freezing test, the cause of the freezing increase zone I cannot be the migration of external moisture into the soil body. The cause of the different phase transition latent heat of water at different refrigeration temperatures and the cause of the freezing increase zone I can only occur inside the soil body.

Then, the various components and possible causes within the soil are analyzed. As shown in Fig. 4, the soil particles consist of mineral particles, bound water, free water and pore gas. According to the theory of diffusion bilayer, the particles have a certain electrical property of their own, which produces a certain adsorption effect on water molecules. According to the different effects of the electrical properties of the particles, free water is hardly affected by adsorption, weakly bound water is affected by some adsorption, and strongly bound water is affected by stronger adsorption. Thus, take the mineral particles as center, from close to far, there are strongly bound water, weakly bound water and free water. Between the mineral particles, there is free water as well as pore gas. Since the soil is a three-phase mixture consisted of mineral particles, water and pore gas, with the mineral particles in the solid phase and the pore gas in the gas phase, the phase change of the mineral particles and pore gas during the cooling process is not considered at present. The lowest temperature of the soil in the three working conditions is −11 °C, and it is obvious that the cause of the freezing increase zone I cannot be caused by the phase transition of bound water to ice.

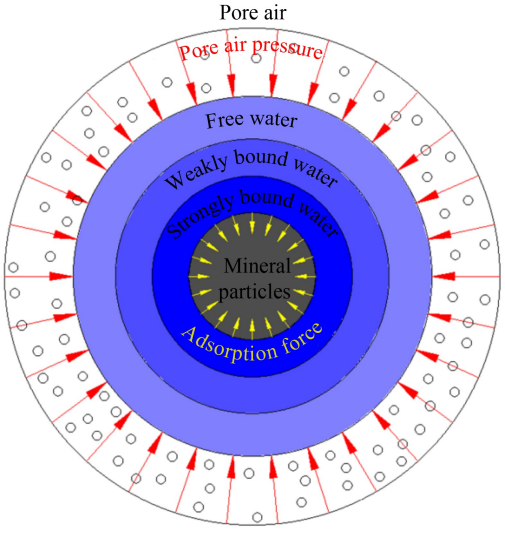

Fig. 4 The relationship between soil particles, pore water, and pore air pressure.

The content of strong bound water in clay minerals is about 30% to 50% [46–48]. The density of bound water is about 1.35 g/cm^3 [49], and the density of free water is about 1.0 g/cm^3.Meanwhile, among the three phases of solid, liquid, and gas, the volume of gas is most affected by temperature. Therefore, for the phenomenon of soil volume increment before free water phase transition freezing in the closed environment freezing test, this issue

proposes a conjecture: as the temperature of the soil decreases, the pore gas pressure gradually decreases, which causes the higher density bound water in the soil to switch to the lower density free water before free water phase transition freezing, which induces the volume increment of the soil before free water phase transition freezing.

3 Air pressure changes in water adsorption isotherm measurements

This section analyses the effect of air pressure on the existence form of water in soil and the magnitude of the influencing air pressure on the classical adsorption isotherm test and an analytical approach.

3.1 Test principle and vapor balance pressure

The water adsorption isotherm measurement is a classical test to study the effect of air pressure changes on the existence form of water in soil under isothermal conditions. As shown in Fig. 5, the specimen was placed in a closed container, and the water vapor in the closed container was adsorbed through the solution concentration, so that the partial pressure of water vapor in the closed environment was less than the partial pressure of saturated water vapor at the same temperature, which in turn made all kinds of water in the mineral particles dissipated gradually. At a certain temperature, mineral particles have a certain adsorption force on water, so there are different thresholds in the dissipation process. The water adsorption isotherm measurement, which uses the relative pressure (p_s/p_0) of water vapor as a variable, is used to study the process of water dissipation in mineral particles. The relative pressure (p_s/p_0) of water vapor, is the ratio of the water vapor partial pressure, p_s of a gas to the partial pressure of water vapor at saturated water vapor, p_0, at the same temperature and atmospheric pressure.

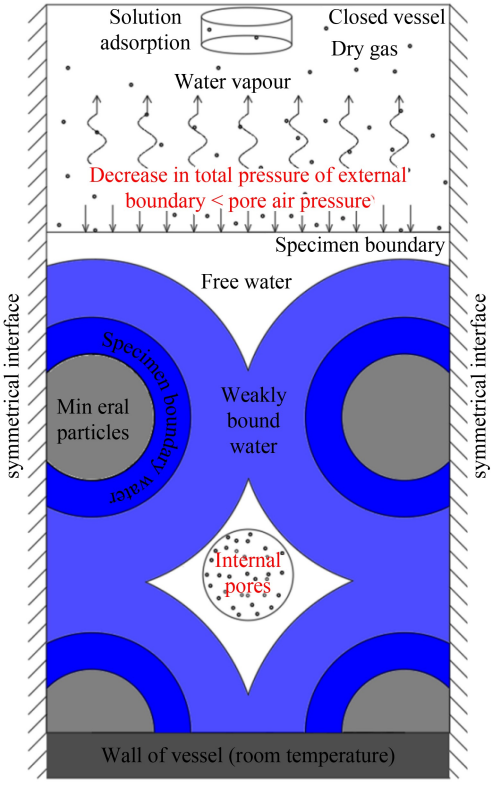

Fig. 5 The principle of the water adsorption isotherm measurement. (Note: The external dry air pressure remains constant, the external water vapor air pressure decreases and the internal pore air pressure in the soil remains constant.)

References [50–53] used the water adsorption isotherm measurements to experimentally test various types of soils, such as artificial trial soil samples, Shaanxi loess, Guangzhou clay, Shanghai clay, Tianjin clay, and Suzhou clay. The same relative pressure (p/p_0) range of water vapor for the water adsorption conditions were given [54–56]. Taking the water adsorption isotherm measurements for Shanxi Fuping loess as an example, the relative pressure of water (p/p_0) in Shanxi Fuping loess were 1, 0.98, 0.90, and 0. That is to say, when the relative pressure (p/p_0) of water was 1, water vapor, free water, weakly bonded water, and strongly bonded water existed at the same time. When the relative pressure (p/p_0) range of water was between 1 and 0.98, free water began to dissipate. When the relative pressure (p/p_0) of water is 0.98, all free water is lost. When the relative pressure (p/p_0) range of water is between 0.98 and 0.90, the weakly bound water starts to be lost. When the relative pressure (p/p_0) of water is 0.90, the weakly bound water is completely lost. When the relative pressure (p/p_0) range of water is between 0.90 and 0, the strongly bound water starts to be lost. And when the relative pressure (p/p_0) of water is 0, the strongly bound water is completely lost.

3.2 Barometric characterization of the relative pressure of water

The container of the water vapor adsorption isotherm measurements is closed and with constant temperature. In this situation, the pores are saturated with water vapor partial pressure of the closed environment, and the dry air partial pressure of the pores is the dry air partial pressure of the closed environment. The isothermal adsorption test in fact maintains the dry air partial pressure unchanged while decreasing the water vapor partial pressure, which ultimately reduces the pore air pressure. In other words, the higher drop in the partial pressure of water vapor in the closed container environment, the smaller the pore air pressure and the higher loss of water vapor from the pore.

According to the three-phase relationship of water, the existence form of water in soil is influenced by both

pressure and temperature factors. The use of the relative pressure of water cannot intuitively reveal the influence of the pressure factor on the existence form of water in soil. To further reveal the influence of pressure on the existence form of water in soil, this study converts the relative pressure of water into air pressure to reformulate the transformation of the existence form of water in soil in the water vapor adsorption isotherm measurement.

In the reformulated test, the water vapor adsorption isotherm measurement conditions were assumed to be room temperature of 25 °C, relative air humidity of 0.4, and 1 standard atmospheric pressure at 0 °C, i.e., 101.325 kPa.

The saturated water vapor pressure was calculated according to Emanuel's empirical formula (Eq. (1)):

$$\ln[p_s(T)] = 53.67957 - \frac{6743.763}{T} - 4.8451 \ln T, \quad (1)$$

$$T = 273.15 + t, \quad (2)$$

where p_s is the actual partial pressure of water vapor, T is the Fahrenheit temperature, t is the Celsius temperature.

The partial pressure of dry air was calculated from the Clapeyron equation (Eq. (3)) for an ideal gaseous state:

$$P_d V_d = n_d R_d T_d, \quad (3)$$

$$\frac{P_{d0}}{T_{d0}} = \frac{P_{d1}}{T_{d1}}, \quad (4)$$

where P_d is the dry air pressure, V_d is the pore volume, n_d is the dry air moles, R_d is the dry air body constant, T_{d0} and T_{d1} are initial temperature and temperature after the change of the dry air, respectively. P_{d0} and P_{d1} are the partial pressure of dry air before and after the temperature change, respectively.

Figure 6 shows the relationship between the pore air pressure, the water vapor partial pressure, and the dry air partial pressure and the relative pressure of water in the water vapor adsorption isotherm measurement. When the relative pressure (p/p_0) of water is 1, i.e., the pore air pressure was 103.352 kPa, free water, weakly bound water and strongly bound water exist simultaneously. When the relative pressure (p/p_0) of water was 0.98, i.e., the pore air pressure was 103.288 kPa, the free water was all dispersed. When the relative pressure (p/p_0) of water was 0.90, i.e., the pore air pressure was 103.035 kPa, the weakly bound water was completely dispersed. When the relative pressure (p/p_0) of water is 0, i.e., the pore air pressure was 100.185 kPa, the strongly bound water was completely dispersed.

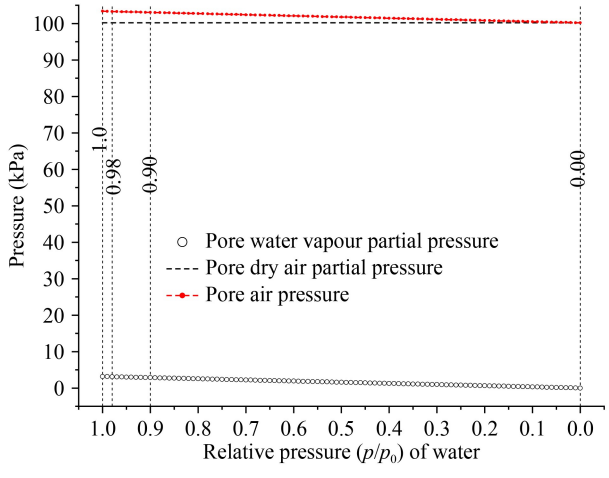

Fig. 6 The relationship between the pore air pressure, the pore water vapor partial pressure, and the pore dry air partial pressure and the relative pressure of water in the water vapor adsorption isotherm measurement.

That is, at 1 standard atmospheric pressure, when the pore air pressure decreases by 0.06 kPa, the free water is completely dispersed. When the pore air pressure decreases by 0.32 kPa, the weakly bound water is completely dispersed. When the pore air pressure decreases by 3.2 kPa, the strongly bound water is completely dispersed. For the water vapor adsorption isotherm measurement, it is found that the pore air pressure had a significant effect on the existence form of water in the mineral particles when the air pressure was used as the measurement index expression.

4 Air pressure changes during soil cooling

In the previous section, the effect of air pressure on the existence form of water in mineral particles and the magnitude of the air pressure values affected were analyzed based on the water vapor adsorption isotherm measurement. In this section, the changes in pore air pressure during soil cooling are analyzed using the analytical method.

4.1 Principles of soil cooling

As shown in Fig. 7, cooling of the soil is usually done by heat conduction or cold radiation. Radiation cooling is used in natural cold weather and in the air cold bath used in the laboratory. Conduction cooling is used in the AGF method, i.e., the circulating fluid is used to cool the tube wall, and then the tube wall cools the soil. Soil cooling, including mineral particle cooling, cooling of water in the soil, and pore gas cooling. In addition, clayey soils are a dense soil structure composed of the microfine mineral particles. For pore gas, it can be considered as a closed environment and pore water vapor can be considered as saturated. The pore air pressure is equal to the sum of the partial pressure of dry air in the pores and the partial pressure of saturated water vapor in the pores.

4.2 Pore air pressure variation

It is assumed that the atmospheric temperature of the soil

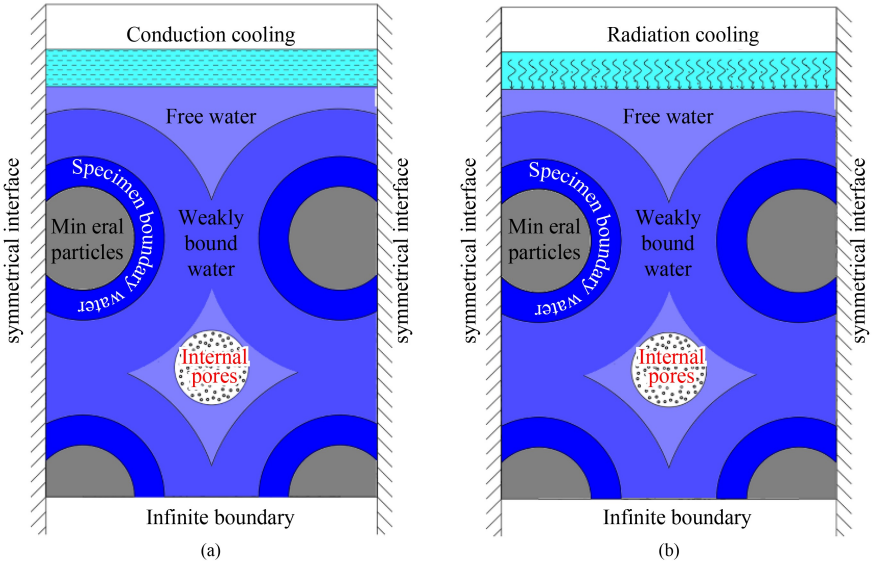

Fig. 7 Schematic diagram of soil cooling principle: (a) conductive cooling; (b) radiation cooling. (Note: The pressure of internal pore air in the soil decreases.)

body before cooling is 25 °C, the relative humidity of the air is 0.4, and the atmospheric standard pressure is 101.325 kPa at 0 °C. The partial pressure of pore dry air, the partial pressure of pore water vapor pressure and the pore air pressure during the cooling process are calculated according to Eqs. (1)–(4). As shown in Fig. 8, the partial pressure of pore dry air, the partial pressure of pore water vapor pressure, and the pore air pressure all decreased substantially as the temperature decreased. In particular, the pore air pressure was lower by about 3.0 and 3.5 kPa when the temperature decreased from 25 to 4 and 0 °C, respectively.

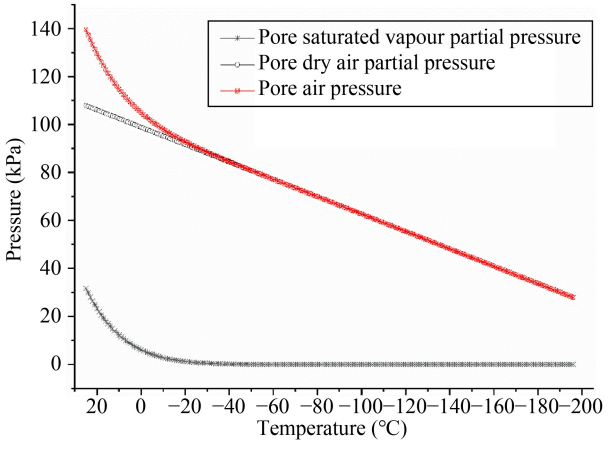

Fig. 8 Relationship between pore air pressure and temperature within a soil body.

4.3 Causes of volume increment in the soil before phase transition freezing of free water

The analysis in Section 3 shows that when the pore air pressure decreases by 0.32 kPa, all the weakly bound water is dissipated. And when the pore air pressure decreases by 3.2 kPa, all the strongly bound water is dissipated. In this section, the study of pore air pressure under cooling shows that when the temperature is lowered from 25 to 4 and 0 °C, the pore air pressure is lower by 3.0 and 3.5 kPa, respectively. It can be concluded that before the soil cools down to the freezing point of free water (0 to 4 °C), all or the vast majority of the bound water has already changed its existence form to free water. Due to the density of bound water and the density of weakly bound water being much greater than that of free water, the volume of the soil occurs in a large volume increment before the free water phase transition freezing.

In addition, it is noted that for the three working conditions Figs. 2(a)–2(c), around 4 °C coincidentally marks the boundary of the freeze-shrink zone. This indicates that the decrease in temperature caused a decrease in pore air pressure, which in turn caused the conversion of bound water into free water, resulting in a structural reorganization of the soil skeleton caused by a decrease in the thickness of the bound water film.

5 Experimental verification

The limitations of current technological means make it difficult to test the bound water transformation during cooling by direct testing. The transformation of bound water into free water before free water phase transitions can in turn cause significant changes in the temperature field and the frost heave amount. Therefore, this study provides an indirect verification of the above conclusions through the temperature field development law.

5.1 Calculation model and basic parameters

1) Three-phase composition model of soil

Figure 9 shows a schematic diagram of the three-phase composition of the soil. The dry soil particles of the geotechnical test are assumed to have a volume of 1 and a pore ratio of e. The dry soil particles consist of mineral particles and strongly bound water. The pore volume consists of pore gas, free water, and all weakly bound water.

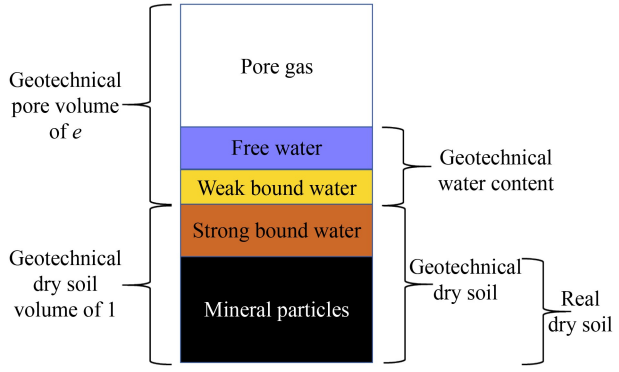

Fig. 9 Schematic diagram of the three-phase composition of the soil.

2) Fundamental assumptions

The following fundamental assumptions are made in the calculation model.

First, the phase transition freezing process of free water obeys the law of conservation of mass.

Secondly, the change in heat when the bound water is converted to free water is much smaller than the value of the latent heat of phase transition and does not affect the law of development of the temperature field.

Thirdly, the heat of phase transition in the conversion of pore water vapor to free water is negligible.

Fourthly, this calculation model did not determine the water content of weakly bound water. The so-called water content is to take the geotechnical test 100–105 °C measured water. The weakly bonded water is regarded as free water in the calculation model. This calculation will cause a certain error, but does not affect the conclusion.

3) The value of the density of water

Studies have shown that the density of ice is about 0.92 g/cm^3, the density of free water is about 1.0 g/cm^3, the density of weakly bound water is about 1.1–1.2 g/cm^3, and the density of strongly bound water is about 1.2–1.5 g/cm^3 [50,57,58]. In the calculation model, the density of ice was taken as 0.92 g/cm^3, the density of free water was 1.0 g/cm^3 and the density of strongly bound water was 1.3 g/cm^3.

4) Strongly bound water content

Reference [59] used soil suction characteristics to show that for the same mass of soil, the plastic-liquid limit is approximately the same for different densities and confining pressures. As the mass water content increases, strongly bound water begins to appear in soil. When the plastic limit is reached, the content of strongly bound water reaches the maximum and weakly bound water begins to appear in soil. The content of weakly bound water reaches the maximum when the liquid limit is reached and free water begins to appear in soil subsequently. With the increase of free water, the soil eventually reaches the saturation state [60,61]. Research results show that the strong bound water is 0.885 times the ratio of the plastic limit water content. In this study, the water content of strongly bound water is calculated according to Eq. (5).

$$w_g = 0.885 w_p, \tag{5}$$

where w_g is the content of strongly bound water and w_p is the content of water at the plastic limit.

5) Real dry soil quality

The specific gravity of dry soil in conventional geotechnical tests is the soil after the removal of free water plus some or all of the weakly bound water, i.e., the mineral particles plus the strongly bound water. In this study, the mineral particles after the complete loss of the strongly bound water are referred to as real dry soil. The ratio of the mass of strongly bound water to the real dry soil is defined as the strongly bound water content. Accordingly, the mass of the real dry soil is calculated in the following way:

$$w_g = \frac{m_g}{m_{ts}} = \frac{\rho_g \cdot v_g}{m_s - \rho_g \cdot v_g} = \frac{\rho_g \cdot v_g}{\rho_w G_s \cdot v_s - \rho_g \cdot v_g}, \tag{6}$$

where m_g is the mass of strongly bound water, m_{ts} is the mass of dry soil at 250 °C, m_s is the mass of dry soil from geotechnical tests, v_s is the volume of dry soil from geotechnical tests, ρ_g is the density of strongly bound water, v_g is the volume of strongly bound water, ρ_w is the density of free water, G_s is the specific gravity of geotechnical test dry soil.

5.2 Temperature field calculation method

In this study, a 3 dimensional (3D) finite element is used to establish the computational model, as shown in Fig. 10. It is divided into quadrilateral second-order cells using the automatic division method, with a total of 2066 elements and 6652 nodes. The constrained boundary conditions are that the upper sandy soil is the stable temperature boundary, and the surrounding box is the adiabatic boundary. The latent heat of phase transition of water is represented by enthalpy change. The numerical calculation boundary conditions are the same as the model testing boundary conditions. The initial ambient temperature is set to 20 °C, and the flow heat transfer coefficient of the soil is set to 10.6 W/(m^2·°C). The

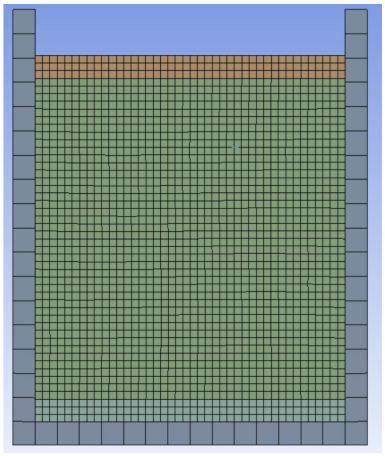

Fig. 10 3D finite element calculation model of temperature field.

boundary between the test chamber and the soil is an adiabatic boundary condition.

The basic physical parameters of loess with a moisture content of 16%, based on tests and calculated, are shown in Table 2 below. The parameters of the sandy soil and the outer frame material of the test chamber are shown in Table 3.

The latent heat of phase transition of water during soil cooling has a great influence on the change of temperature field during the whole process of soil freezing. Studies have shown that the content of unfrozen water is always in dynamic equilibrium with the negative temperature [62,63], as shown in Eqs. (7)–(9).

$$\omega_{\mathrm{u}} = A_{\mathrm{f}}^{-B}, \tag{7}$$

$$A = \omega_{\mathrm{L}} T_{\mathrm{L}}^{B}, \tag{8}$$

Table 2 Physical parameters of loess

Material name	Loess
water content (%)	16
Maximum dry density (kg/m^3)	1.78×10^3
Density (kg/m^3)	1.883×10^3
Plastic limit water content (%)	15.21
Liquid limit water content (%)	28.38
Real water content (%)	35.948
Specific gravity (G_{s})	2.71

Table 3 Physical parameters of sandy soil and model box

Material name	Sandy soil	Model box
Elastic modulus (MPa)	20	2×10^5
Density (kg/m^3)	1480	7850
Poisson's ratio	0.25	0.3
specific heat capacity (J/(kg·°C))	920	434
Thermal conductivity (W/(m·°C))	1	50

$$B = \frac{\ln \omega_{\mathrm{L}} - \ln \omega_{\mathrm{p}}}{\ln T_{\mathrm{p}} - \ln T_{\mathrm{L}}}, \tag{9}$$

where ω_{u} is the content of unfrozen water, ω_{p} is the content of plastic limit water, ω_{L} is the content of liquid limit water, T_{f} is the absolute value of freezing temperature at the plastic limit, T_{L} is the absolute value of freezing temperature at the liquid limit.

The latent heat of phase transition of soil can be calculated by the following empirical formula:

$$Q = L r_{\mathrm{d}} (\omega - \omega_{\mathrm{u}}), \tag{10}$$

$$r_{\mathrm{d}} = \frac{d_{\mathrm{s}} r_{\omega}}{1 + d_{\mathrm{s}} \omega}, \tag{11}$$

where Q is the latent heat of phase transition, L is the latent heat of crystallization and thawing of water, which is empirically assumed to be 334.56 kJ/kg, ω is the content of water in soil, ω_{u} is the content of unfrozen water, r_{d} is the dry density of soil, r_{ω} is the density of water, d_{s} is the relative density of soil.

5.3 Analysis of results

In this study, the temperature measurement points in the middle of the test model box shown in Fig. 1 are selected to demonstrate the development law of temperature field. Figures 11(a)−11(c) show the development pattern of temperature field considering only free water, bound water transformation and test values. The curves with solid black markers are the test values of soil temperature (hereinafter referred to as test values). The curves with red line markers are the calculated values considering the transformation of bound water into free water participating in the latent heat of phase transition (hereinafter referred to as calculated values considering bound water). And the curves with hollow pink markers are the calculated values considering only the original free water participating in the latent heat of phase transition (hereinafter referred to as calculated values considering only free water).

As it could be seen from Figs. 11(a)−11(c), the temperature-time trends of the experimental values of soil temperature, the calculated values on the bound water, and the calculated values on only the free water were similar, and all of them were gradually decreasing with time, and showed a rapid temperature decrease zone, an approximate plateau period, and a slow decrease zone. The difference lies in the fact that in the above three zones, the calculated values considering only free water showed higher difference from the experimental values from the beginning to the end, whereas the calculated values on bound water were less from the experimental values from the beginning to the end. In particular, in the zone of rapidly decreasing temperature, the approximate

plateau period and the calculated values considering bound water were in consistence with the experimental values.

As shown in Table 4, when only free water was considered, the maximum calculation error of icing temperature was 9.2 °C, the maximum moment error was 16.1%, and the maximum temperature error at the end of the approximate plateau period was 18.1 °C, the maximum moment error was 51.9%. When the bound water was considered, the maximum calculation error in icing temperature was 0.8 °C, the maximum moment error was 5.6%, and the maximum temperature error at the end of the approximate plateau period was 0.8 °C, the maximum moment error was 0%. The calculation accuracy of the icing temperature was improved by 8.4 °C and 10.5% of the moment of occurrence when considering bound water, and the calculation accuracy of the temperature at the end of the approximate plateau period was improved by 17.3 °C and 51.9% of the moment of occurrence compared with that of free water only.

From the above analysis, it could be seen that the calculation error in the temperature field is very large when only free water is considered, while the calculation error in the temperature field is much smaller when bound water is considered. In particular, in the rapid temperature drop zone and the approximate plateau period, when the latent heat of phase transition of the bound water into free water is considered, the calculated values of the temperatures highly coincide with the experimental values, and the length of the approximate plateau period highly coincides with the experiments.

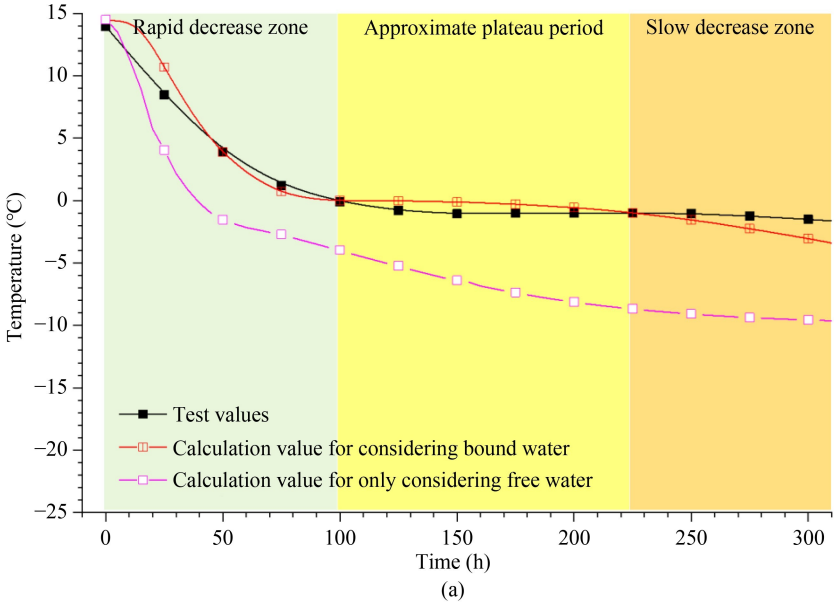

(a)

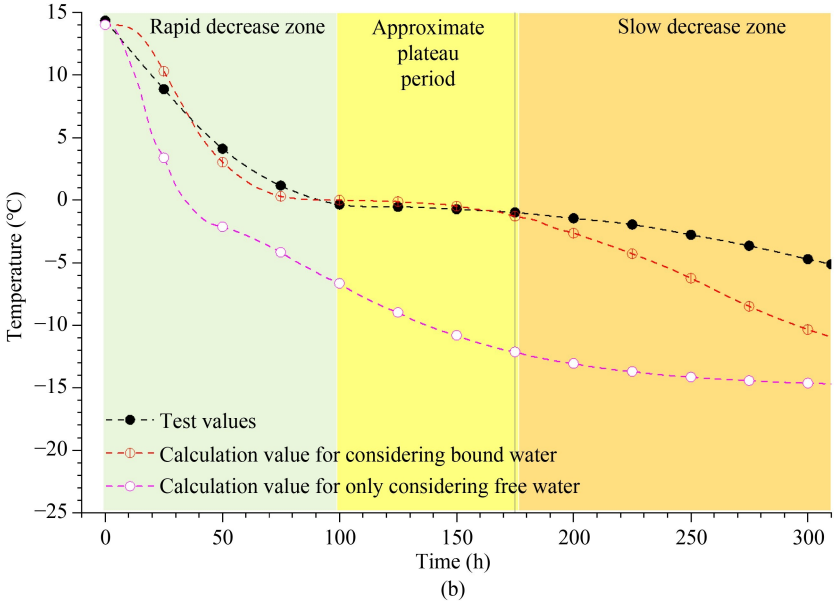

(b)

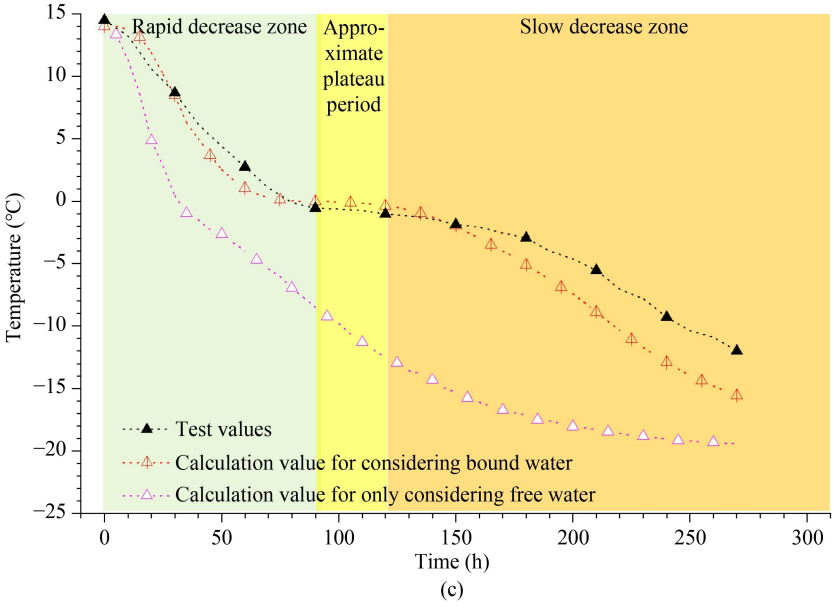

Fig. 11 The law of temperature field development for combined water transformations considered: (a) working condition 1: 16% water content, temperature load −10° C; (b) working condition 2: 16% water content, temperature load −15 °C; (c) working condition 3: 16% water content, temperature load −20 °C.

Table 4 Critical calculated values and errors for temperature fields

Refrigeration working conditions comparison content	Category	Freezing temperature				Temperature at the end of the approximate plateau period			
		temperature		moment		temperature		moment	
		value (°C)	error (°C)	value (h)	error (%)	value (°C)	error (°C)	value (h)	error (%)
Work condition 1	considering only free water	−1.5	−1.4	50	16.1	−9.1	−8.1	250	8.1
	considering bound water	0	0.1	100	0	−1.0	0	225	0
	experimental value	−0.1	–	100	–	−1.0	–	225	–
Work condition 2	considering only free water	−2.1	−1.7	50	11.3	−14.1	−13.1	250	24.2
	considering bound water	−0.3	0.1	85	4.8	−1.3	−0.3	175	0
	experimental value	−0.4	–	100	–	−1	–	175	–
Work condition 3	considering only free water	−9.7	−9.2	35	14.8	−19.3	−18.1	260	51.9
	considering bound water	0.3	0.8	75	5.6	−0.4	0.8	120	0
	experimental value	−0.6	–	90	–	−1.2	–	120	–
Maximum error	considering only free water	–	9.2	–	16.1	–	18.1	–	51.9
	considering bound water	–	0.8	–	5.6	–	0.8	–	0

Note: In this table, moment error = (moment calculated value−moment test value)/total time.

This indicates that the bound water has been converted to free water before the free water phase transition.

In the zone of slowly decreasing temperature, the calculated value with the bound water also shows a large difference from the experimental value, and the error increases with the rise in the cooling time. The reasons for this can first be the formation of a more stable ice skeleton system after a complete frozen of all the free water by phase transition. As the temperature continues to decrease, the pore air pressure will continue to decrease along, which may further cause stronger adsorption of bound water or other forms of water into the free water phase transition icing. Secondly, the calculation method of unfrozen water content in this study is based on the classical formula, which may be different from the case of considering the transformation of bound water.

6 Discussion

6.1 The most important finding in the study

Under the background of the disconnection between the current theoretical knowledge of the existence form of

water in soil disciplines and the engineering practice, and starting from the interesting phenomenon of the volume increment before the free water phase transition in the closed-environment permafrost test, a combination of proposed conjectures, theoretical analyses, numerical calculation, and indoor experiments was adopted to reveal the mechanism of the effect of pore pressures on the existence form of water in soil, and to put forward the viewpoint that the bound water is transformed to free water before the free water phase transition.

6.2 Significance of the study

The content of water and unfrozen water in soil (the content of unfrozen water actually is to calculate the amount of water that can participate in freezing) are the most fundamental parameters in permafrost science. Currently, the content of water in soil obtained from the result of 105−110 °C drying test is adopted as the fundamental parameter in permafrost science, and the theoretical cognition of present permafrost science is that the water involved in freezing is only free water and a small portion of weakly bound water. In this study, the theory that the bound water transforms into free water before the phase transition of free water is proposed, and it is pointed out that the water content that can participate in freezing should encompass free water, weakly bound water and strongly bound water. On the basis of this study, it indicates a possibility of modification on the related theory, calculation, engineering application, and specification in permafrost science.

First, the findings of this study are of direct importance to theoretical research and engineering practice in the field of freezing methods. Because of the failure to consider the bonded water transformation problem, the freezing temperature calculated according to the formula of the theoretical research considering only the free water is bound to deviate far from the actual freezing temperature. That is to say, the frozen soil thickness that is considered theoretically reached, but unfrozen soil appears in the actual excavation. This will inevitably lead to the over-conservative design relying on experience and prolonged term in freezing construction. Considering the bound water transformation phenomenon, it will make the temperature calculation results through the theoretical study more in agreement with the actual temperature, and will solve the problem of over-conservative design and shorten the prolonged construction periods. This will drastically reduce the manpower, materials and energy and make the freezing method more green and low-carbon.

Secondly, the findings of this study are important for the development of the freezing mechanism in permafrost. In the original freezing theory, phase transition icing is caused by only free water and a small amount of weakly bound water. This study presents a new theoretical perspective that bound water is transformed to free water to participate in phase transition icing, which is an enrichment and development of the original freezing theory. The freezing theory, inevitably, produces a series of improvements and advances. For example, when free water and a small amount of weakly bound water are considered as the water involved in the phase transition, the water content determination of the drying test at 105 to 110 °C will be used as the basic parameter of permafrost science. However, it is actually free water, weakly bound water, and strongly bound water as the water that can participate in the phase transition, and in this case the temperature of complete water loss of bound water must be used for the drying test.

Thirdly, in permafrost science, the findings of this study are critical to the research of frost heaving mechanisms and frozen disaster management. The original freezing theory suggests that the main reason for generating a large amount of frost heave is the segregation frost heave by external water migration. In the closed environment freezing test of this study, the volume increment before the phase transition of free water has reached 52% to 82% of the total frost heaving volume, indicating that the other main cause of frost heave originates from the inside. This theoretical cognition from this study will provide new insights for research and measures for frozen disaster management. In addition, when the mechanism cognition of bound water transformation is adopted, the problem of the inability to calculate the amount of frost heave will be solved. Due to the space limitation, the study of the calculation method of frost heaving volume will be introduced in the future research.

6.3 Limitations of the findings in this study

1) The closed environment freezing test was conducted for diverse refrigeration conditions. However, it only focused on one type of loess soil. To examine whether similar occurrences arise for other soil types or substances, the research team will carry out in future research.

2) During the analysis of the adsorption isotherm test, it was assumed that the testing environment was at one standard atmosphere and the temperature of 25 °C, which may differ from the actual situation. However, it does not affect the quantitative and qualitative analyses of the pore air pressure on the existence form of water in soil.

3) When analyzing the air pressure during the cooling process of the soil, it is assumed that the test environment is at a standard atmosphere of 1 and the temperature of 25 °C. Additionally, it is assumed that the pores in the soil are closed, which may be different from the actual situation. However, it does not affect the quantitative and

qualitative analyses of pore air pressure during the cooling process.

7 Conclusions

1) Based on freezing tests in confined environments, it was proposed that a decrease in the temperature of the soil causes a decrease in the pore air pressure then leads to the conversion of the bound water to free water before the free water phase transition is achieved. Freezing tests in closed environments have established a uniform curve of frost heave amount-temperature-time. The interesting phenomena of a large volume increment before free water phase transition freezing and a longer phase transition plateau period at lower soil temperatures have been found. The lower the soil temperature, the larger the proportion of the volume increment before free water phase transition freezing in the total volume increment. At soil temperatures around −12 °C, the volume increment before free water phase transition freezing accounts for 82% of the total volume increment.

2) For the classical water adsorption isotherm measurements, it was reformulated from the perspective of air pressure to reveal the mechanism of pore air pressure on the existence form of water in mineral particles. Under standard atmospheric pressure, free water is dispersed when the pore air pressure decreases by 0.06 kPa. The weakly bound water is completely dispersed when the pore air pressure decreases by 0.32 kPa. The strongly bound water is completely dispersed when the pore air pressure decreases by 3.2 kPa.

3) Pore air pressure was analyzed for both natural and artificially cooled modes of soil cooling to reveal the mechanism of the effect of soil cooling on pore air pressure, and the possibility of a decrease in pore air pressure due to soil cooling, which in turn leads to the conversion of bound water to free water and the occurrence of a volume increment prior to the free-water phase transition. At a pressure of 1 standard atmosphere, the pore air pressure decreases by about 3.0 and 3.5 kPa when the temperature decreases from 25 to 4 and 0 °C, respectively. And before the soil cooled down to the free water freezing point (0–4 °C), all or most of the bound water has already undergone the transformation of its existence form and become free water. Since the density of bound water and the density of weakly bound water is much greater than that of free water, it causes a large volume increment to occur in the volume of the soil before the free water phase transition freezing.

4) The calculation and analysis of the temperature field considering the bound water verifies the presumption that the bound water transforms into free water before the free water phase transition. Considering that the bound water transforms into free water before the phase transition of free water, the calculated values of the soil temperature development pattern are in high agreement with the test values. When considering bound water, the maximum computational error in freezing temperature is 0.8 °C and the maximum moment error is 5.6%. Similarly, the maximum temperature error at the end of the approximate plateau period is 0.8 °C and the maximum moment error is 0%. The calculation accuracy of the icing temperature has been improved by 8.4 °C and 10.5% of the moment of occurrence when considering bound water, and the calculation accuracy of the temperature at the end of the approximate plateau period is improved by 17.3 °C and 51.9% of the moment of occurrence compared with that of free water only.

Acknowledgements This work was supported by the National Natural Science Foundation of China (Grant Nos. 42407226 and 51978431). The authors gratefully acknowledge the financial support.

Competing interests The authors declare that they have no competing interests.

References

1. Palmer A C, Williams P J. Frost heave and pipeline upheaval buckling. Canadian Geotechnical Journal, 2003, 40(5): 1033–1038
2. Hotineanu A, Bouasker M, Aldaood A, Al-Mukhtar M. Effect of freeze–thaw cycling on the mechanical properties of lime-stabilized expansive clays. Cold Regions Science and Technology, 2015, 119: 151–157
3. Yu F, Qi J L, Lai Y M, Sivasithamparam N, Yao X L, Zhang M Y, Liu Y Z, Wu G L. Typical embankment settlement/heave patterns of the Qinghai−Xizang highway in permafrost regions: Formation and evolution. Engineering Geology, 2016, 214: 147–156
4. Xiang B, Liu E L, Yang L X. Influences of freezing–thawing actions on mechanical properties of soils and stress and deformation of soil slope in cold regions. Scientific Reports, 2022, 12(1): 5387
5. He J, Yao J, Chen X, Liu F, Zhu H. Do civil engineering fronts emerge from interdisciplinary research? Frontiers of Structural and Civil Engineering, 2023, 17(1): 1–9
6. Song S, Wang P, Yin Z, Cheng Y P. Micromechanical modeling of

hollow cylinder torsional shear test on sand using discrete element method. Journal of Rock Mechanics and Geotechnical Engineering, 2024, 16(12): 5193–5208
7. Marwan A, Zhou M, Abdelrehim M, Meschke G. Optimization of artificial ground freezing in tunneling in the presence of seepage flow. Computers and Geotechnics, 2016, 75: 112–125
8. Harris J S. Ground Freezing in Practice. London: Thomas Telford, 1995
9. Alzoubi M A, Xu M H, Hassani F P, Poncet S, Sasmito A P. Artificial ground freezing: A review of thermal and hydraulic aspects. Tunnelling and Underground Space Technology, 2020, 104: 103534
10. Zhang Q, Liu Y, Dai F. A frost heave pressure model for fractured rocks subjected to repeated freeze-thaw deterioration. Engineering Geology, 2024, 337: 107587
11. Braun B, Shuster J, Burnham E. Ground freezing for support of open excavations. Engineering Geology, 1979, 13(1–4): 429–453
12. Hu X D, Deng S J, Wang Y. Test investigation on mechanical behavior of steel pipe-frozen soil composite structure based on Freeze-Sealing Pipe Roof applied to Gongbei tunnel. Tunnelling and Underground Space Technology, 2018, 79: 346–355
13. Wei Y, Tang C S, Zhu C, Cheng Q, Lu Y, Li L, Tian B G, Shi B. Influence of desiccation during freeze–thaw cycles on volumetric shrinkage and tensile strength of compacted clayey soils. Engineering Geology, 2024, 334: 107513
14. Gilpin R R. A model for the prediction of ice lensing and frost heave in soils. Water Resources Research, 1980, 16(5): 918–930
15. Nassr A, Esmaeili-Falak M, Katebi H, Javadi A. A new approach to modeling the behavior of frozen soils. Engineering Geology, 2018, 246: 82–90
16. Li T, Zhou Y, Shi X Y, Hu X X, Zhou G Q. Analytical solution for the soil freezing process induced by an infinite line sink. International Journal of Thermal Sciences, 2018, 127: 232–241
17. Hong Z Q, Hu X D, Zhang J. Mathematical model of temperature field and its analytical solution for Freeze-Sealing Pipe-Roof method induced by radial offset of adjacent jacking pipes. Cold Regions Science and Technology, 2023, 205: 103699
18. Niggemann K, Fuentes R. New semi-analytical approach for ice lens heaving during artificial freezing of fine-grained material. Journal of Rock Mechanics and Geotechnical Engineering, 2023, 15(11): 2994–3009
19. Gallardo A H, Marui A. The aftermath of the Fukushima nuclear accident: measures to contain groundwater contamination. Science of the Total Environment, 2016, 547: 261–268
20. Alzoubi M A, Zueter A, Nie-Rouquette A, Sasmito A P. Freezing on demand: a new concept for mine safety and energy savings in wet underground mines. International Journal of Mining Science and Technology, 2019, 29(4): 621–627
21. Liu Z, Liu J, Li X, Fang J. Experimental study on the volume and strength change of an unsaturated silty clay upon freezing. Cold Regions Science and Technology, 2019, 157: 1–12
22. Zhang D, Li X, Li X K, Zheng S F, Liu A Q, Wang M. Experimental study on the influence of initial water saturation on segregation frost-heaving behavior in silty clay columns. Applied Thermal Engineering, 2023, 234: 121236
23. Hillel D. Fundamentals of Soil Physics. London: Academic Press, 1980
24. Yershov E D. General Geocryology. Cambridge: Cambridge University Press, 1998
25. Wettlaufer J S. Surface phase transitions in ice: from fundamental interactions to applications. Philosophical Transactions-Royal Society. Mathematical, Physical, and Engineering Sciences, 2019, 377(2146): 20180261
26. Hoekstra P. Moisture movement in soils under temperature gradients with the cold-side temperature below freezing. Water Resources Research, 1966, 2(2): 241–250
27. Fukuda M, Orhun A, Luthin J N. Experimental studies of coupled heat and moisture transfer in soils during freezing. Cold Regions Science and Technology, 1980, 3(2–3): 223–232
28. Mironov V, Savin I, Lukin Y, Karavaisky A. Phase transition analysis in freezing moist soils carried out on the basis of phase transitions characteristic to the different types of soil water. In: Proceedings of 2012 IEEE International Geoscience and Remote Sensing Symposium. Munich: IEEE, 2012, 4497–4500
29. Chen Y Q, Zhou Z F, Wang J G, Zhao Y, Dou Z. Quantification and division of unfrozen water content during the freezing process and the influence of soil properties by low-field nuclear magnetic resonance. Journal of Hydrology, 2021, 602: 126719
30. Baker R, Frydman S. Unsaturated soil mechanics: Critical review of physical foundations. Engineering Geology, 2009, 106(1–2): 26–39
31. Li X, Li X. A soil freezing–thawing model based on thermodynamics. Cold Regions Science and Technology, 2023, 211: 103867
32. Li X, Zheng S, Wang M, Liu A. The prediction of the soil freezing characteristic curve using the soil water characteristic curve. Cold Regions Science and Technology, 2023, 212: 103880
33. Lee S, Lee J. Adsorption of water molecules on clay minerals: A molecular dynamics study. Journal of Colloid and Interface Science, 2020, 564: 94–102
34. Zhang Y, Wang F. Effect of clay mineralogy on the adsorption of water and ions in soils. Geoderma, 2021, 380: 114660
35. Williams P J. Unfrozen water content of frozen soils and soil moisture suction. Geotechnique, 1964, 14(2): 133–142
36. Azmatch T F, Sego D C, Arenson L U, Biggar K W. Using soil freezing characteristic curve to estimate the hydraulic conductivity function of partially frozen soils. Cold Regions Science and Technology, 2012, 83–84: 103–109
37. Razumova L A. Basic principles governing the organization of soil moisture observations. Hydrology, 1965, 68: 491–501
38. Liu J, Zhang W, Cui J, Ren Z, Wang E, Li X, Wei G, Tian Y, Ji J, Ma J et al. Extreme low-temperature freezing process and characteristic curve of icy lunar regolith simulant. Acta Astronautica, 2023, 202: 485–496
39. Rempel A W, Worster M G, Wettlaufer J S. Interfacial premelting and the thermomolecular force: Thermodynamic buoyancy. Physical Review Letters, 2001, 87(8): 088501
40. An N, Tang C S, Xu S K, Gong X P, Shi B, Inyang H I. Effects of soil characteristics on moisture evaporation. Engineering Geology, 2018, 239: 126–135
41. Tian H H, Wei C F, Wei H Z, Zhou J Z. Freezing and thawing characteristics of frozen soils: Bound water content and hysteresis

phenomenon. Cold Regions Science and Technology, 2014, 103: 74–81
42. Wettlaufer J S, Worster M G. Premelting dynamics. Annual Review of Fluid Mechanics, 2006, 38(1): 427–452
43. Zhang Z. Study on frost heave characteristics of loess in Lanzhou region under one-dimensional freezing condition. Thesis for the Master's Degree. Lanzhou: Lanzhou Jiaotong University, 2020
44. Liu G. Experimental study on freeze–thaw and strength characteristics of Jiangxi red-clay due to artificial ground freezing. Thesis for the Master's Degree. Nanchang: East China University of Technology, 2022
45. Shang F, Yang C S, Zhang L H, Zhou C L, Han D W, Shi Y J. Analysis of influencing factors of clay particle diffusion in electric double layer. Journal of Glaciology and Geocryology, 2022, 44(2): 495–505
46. Yuan J B. The study for properties of bound water on clayey soils and their quantitative methods. Thesis for the Master's Degree. Guangzhou: South China University of Technology, 2012
47. Song Y P. Influence of bound water on physical and mechanical properties of loess. Thesis for the Master's Degree. Xi'an: Chang' an University, 2018
48. Wang Y J, Hu L M, Yin Z Y. Identification and quantification of soil water components in kaolin by thermogravimetric and kinetic analysis. Engineering Geology, 2023, 324: 107273
49. Zymnis D M, Whittle A J, Germaine J T. Measurement of temperature-dependent bound water in clays. Geotechnical Testing Journal, 2018, 42(1): 232–244
50. Wang P Q. The study for quantitative analysis of water absorbed on clays and their hydration mechanism. Dissertation for the Doctoral Degree. Chengdu: Southwest Petroleum University, 2001
51. Wang T H, Li Y L, Su L J. Types and boundaries of bound water on loess particle surface. Chinese Journal of Geotechnical Engineering, 2014, 36(05): 942–948 (in Chinese)
52. Wu Q. Research on influence of bond water on secondary consolidation and long term strength of soft clay. Dissertation for the Doctoral Degree. Changchun: Jilin University, 2015
53. Zhang R, Xiao Y P, Wu M L, Zheng J L, Milkos B C. Measurement and engineering application of adsorbed water content in fine-grained soils. Journal of Central South University, 2021, 28(5): 1555–1569
54. Kosmas C, Danalatos N G, Poesen J, Wesemael B V. The effect of water vapour adsorption on soil moisture content under Mediterranean climatic conditions. Agricultural Water Management, 1998, 36(2): 157–168
55. Kosmas C, Marathianou M, Gerontidis S, Detsis V, Tsara M, Poesen J. Parameters affecting water vapor adsorption by the soil under semi-arid climatic conditions. Agricultural Water Management, 2001, 48(1): 61–78
56. Prost R, Koutit T, Benchara A, Huaed E. State and location of water adsorbed on clay minerals: Consequences of the hydration and swelling−shrinkage phenomena. Clays and Clay Minerals, 1998, 46(2): 117–131
57. Wu F C. Some characteristics of adsorption combined with water measurement and seepage in cohesive soil. Chinese Journal of Geotechnical Engineering, 1984, 06: 84–93 (in Chinese)
58. Wu F C. Calculation of soil moisture characteristic curve under low suction. Journal of Hydraulic Engineering, 1986, 7: 49–55
59. Zhang H W. Research of the method on determining Atterberg limits of soil by suction stress characteristic curve. Thesis for the Master's Degree. Lanzhou: Lanzhou University of Technology, 2017
60. Davidson D T, Sheeler J B. Clay fraction in engineering soils: III–Influence of amount on properties. Highway Research Board Proceedings, 1952, 31
61. Lu N, Likos W J. Suction stress characteristic curve for unsaturated soil. Journal of Geotechnical and Geoenvironmental Engineering, 2006, 132(2): 131–142
62. Qin Y H, Zhang J M, Zheng B, Qu G Z. The relationship between unfrozen water content and temperature based on continuum thermodynamics. Journal of Qingdao University (Engineering & Technology Edition), 2008, 1: 77–82
63. Li D Y. The experiment and theoretical research on a new test method to measure unfrozen water content in frozen soil. Dissertation for the Doctoral Degree. Beijing: China University of Mining & Technology, 2011